Quantum loops in radiative decays of the a_1 and b_1 axial-vector mesons

L. Roca[1], A. Hosaka[2] and E. Oset[3]

[1] *Departamento de Física. Universidad de Murcia. E-30071 Murcia. Spain*

[2] *Research Center for Nuclear Physics (RCNP), Ibaraki, Osaka 567-0047, Japan*

[3] *Departamento de Física Teórica and IFIC, Centro Mixto Universidad de Valencia-CSIC, Institutos de Investigación de Paterna, Aptdo. 22085, 46071 Valencia, Spain*

February 2, 2008

Abstract

A previous model where the low-lying axial-vector mesons are dynamically generated, implementing unitarity in coupled channels in the vector-pseudoscalar (VP) meson interaction, is applied to evaluate the decay widths of the $a_1(1260)$ and $b_1(1235)$ axial-vector mesons into $\pi\gamma$. Unlike the case of the a_1, the b_1 radiative decay is systematically underestimated at tree level. In this work we evaluate for the first time the loop contribution coming from an initial VP vertex. Despite the large superficial divergence of the loops, the convergence of the relevant loops can be established by using arguments of gauge invariance. The partial decay widths obtained agree with the experimental values within uncertainties, and we show that the loop contribution is crucial in the b_1 case and also important for the a_1 case.

1 Introduction

The unitary extensions of chiral perturbation theory (χPT) have allowed to extend the range of energies where the hadron interaction can be studied. At the same time they have also shown that many meson and baryon resonances are dynamically generated and can be interpreted as quasibound states of pairs of hadrons in coupled channels [1]. A case very well studied is the one of the interaction of the octet of pseudoscalar mesons [2–6] from where a nonet of scalar mesons are generated. Much less studied is the case of the interaction of vector mesons with pseudoscalar mesons, where two independent works [7,8] have shown that the axial vector mesons can be generated dynamically. This novel idea should be confronted with experiment to test the accuracy of its predictions. Some of these predictions have already been tested in Ref. [9]. Contrary to other pictures like quark models, where external sources are coupled to the quarks, in the dynamically generated

picture one assumes that the largest weight of the wave function is due to the two meson cloud, and consequently, the coupling of external sources proceeds via the coupling to the meson components. One interesting test which brings light into this issue is the radiative decay of the resonances. This is the purpose of the present work where we concentrate on the radiative decay of the b_1^+ and a_1^+ axial vectors into $\pi^+\gamma$. The a_1^+ radiative decay has been studied within different contexts, for instance vector meson dominance is used in [10, 11], relating the radiative decay with the $\rho\pi$ decay of the a_1^+. Chiral Lagrangians with vector meson dominance (VMD) are also used in [12] to obtain the radiative width of $a_1^+ \to \pi^+\gamma$. An SU(3) symmetric Lagrangian is used in [13] to account for strong decays of the axial vector mesons and by means of VMD the amplitude for $a_1^+ \to \pi^+\gamma$ is studied and related to the one of [12]. A common feature of these works is that the $b_1^+ \to \pi^+\gamma$ reaction is not discussed and its evaluation in [13] using VMD along the same lines as the $a_1^+ \to \pi^+\gamma$ gives rise to a decay rate substantially smaller than experiment. The $b_1^+ \to \pi^+\gamma$ decay is also neglected in the analysis of [11] citing the small rates obtained.

The rates of $a_1^+ \to \pi^+\gamma$ and $b_1^+ \to \pi^+\gamma$ are also evaluated in [14] using quark models for the $a_1 \to \pi\rho$ and $b_1 \to \pi\omega$ and VMD to relate these amplitudes with the radiative decay. It is emphasized there that because of the factor 1/3 of the $\omega\gamma$ coupling relative to the one of $\rho\gamma$ there is a reduction factor of 1/9 for the radiative decay $b_1^+ \to \pi^+\gamma$ compared to that of the $a_1^+ \to \pi^+\gamma$ decay, resulting in a ratio of these two rates in contradiction with experiment (this is the same argument found in [13] as responsible for the small rate of the $b_1^+ \to \pi^+\gamma$ decay).

In the present work we shall also use the tree level VMD amplitudes, but in addition, the nature of the axial vector mesons as dynamically generated resonance provides a strong coupling to $K^*\bar{K}$ and $\bar{K}^*K$, and subsequent loops with these intermediate states and the photon emitted from these constituents should be considered. We show that the loops are very important, particularly for the case of the $b_1^+ \to \pi^+\gamma$ decay, and the simultaneous consideration of the VMD amplitudes at tree level and loop contributions leads to a good description of both radiative decays.

We shall also show some technical details involving loops with vector mesons. Using arguments of gauge invariance and the Feynman parametrization, one can prove that the loops involving one vector meson and two pseudoscalar mesons are finite, in spite of the large degree of superficial divergence. This was found in [15–18] with the loops involved in radiative decay of the ϕ containing three pseudoscalar mesons.

2 Formalism

In Ref. [8] most of the low-lying axial vector mesons were dynamically generated from the s-wave interaction of the octet of vector-mesons with the octet of pseudoscalar-mesons by using the techniques of the chiral unitary theory. With the only input of a chiral Lagrangian for a vector and pseudoscalar (VP) mesons and the implementation of unitarity in coupled channels, these resonances show up as poles in the second Riemann sheet of the unitarized scattering amplitudes. By evaluating the residues of the scattering amplitudes at the

pole positions, the couplings of the dynamically generated axial-vector resonances to the different VP channels can be obtained. By using these couplings, we found a nice agreement with the experimental VP partial decay rates, despite the fact that no parameters were fitted to experimental data of the axial-vector mesons.

In view of the dominant contribution of the VP channels in the building up and decay of the axial-vector resonances, our starting point to study the radiative decay of the b_1 and a_1 is the transition of these resonances into the allowed VP channels and attaching the photon to the relevant meson lines and vertices. The first kind of mechanisms considered are the

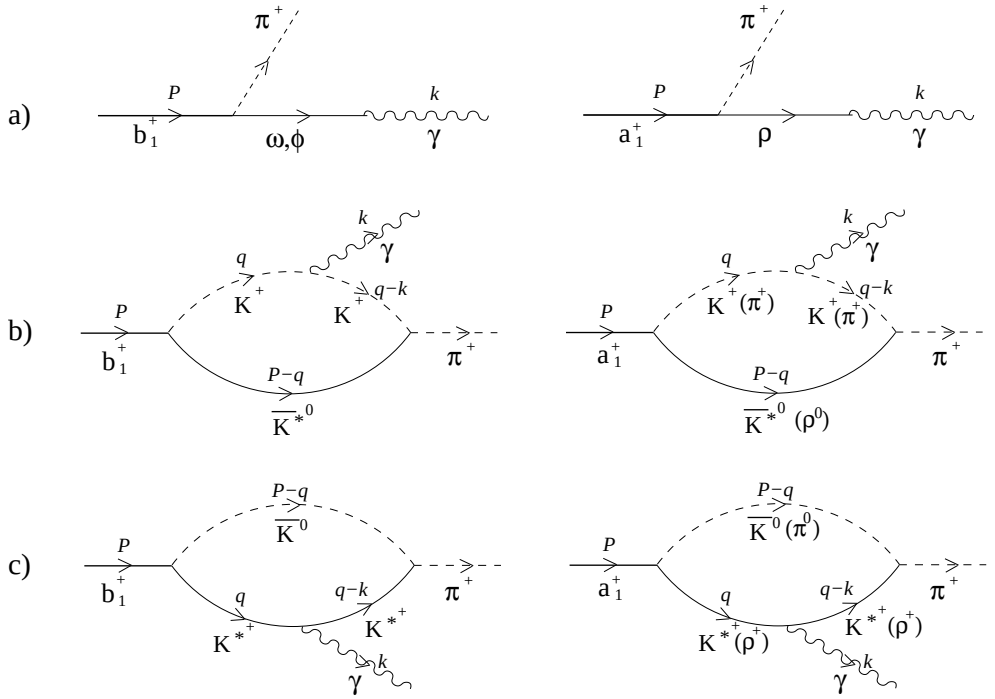

Figure 1: Feynman diagrams contributing to the radiative axial-vector meson decay.

tree level vector meson dominance (VMD) contributions, shown in Fig. 1a). Furthermore, the radiative decay can also proceed from loops of the VP pair with the photon emitted from either the pseudoscalar or the vector meson leg, Fig. 1b) and c). A diagram with the photon directly emitted from the VPP vertex is needed to ensure gauge invariance, but we will explain later on (after Eq. (26)) that, using arguments of gauge invariance, we do not need to evaluate it directly. On the other hand, another kind of loops containing the $VP\gamma$ and VVP vertices is also possible, however, they involve two abnormal intrinsic parity vertices, and hence its contribution should be rather small compared to those already considered. This is indeed the case in the analogous loops present in the radiative decay of the ϕ meson, as it was found in [19].

The intermediate VP states possible in the loops are those used in Ref. [8] to build up the axial vector mesons. These are, for the b_1: $1/\sqrt{2}(\bar{K}^*K + K^*\bar{K})$, $\phi\pi$, $\omega\pi$, $\rho\eta$, and for

the a_1:$1/\sqrt{2}(\bar{K}^*K - K^*\bar{K})$, $\rho\pi$. Note however, that the coupling of the $\phi\pi$, $\omega\pi$, $\rho\eta$ to the final pion violates $G-$parity and hence these channels do not contribute to the b_1 radiative decay. Thus, only the diagrams in Fig. 1 must be evaluated.

Let us start with the evaluation of the tree level contributions. For the $V\gamma$ vertex we use the amplitude

$$t_{V\gamma} = -e\lambda_V \, F_V \, M_V \, \epsilon_V \cdot \epsilon \tag{1}$$

with $\lambda_V = 1,\ 1/3,\ -\sqrt{2}/3$ for ρ, ω and ϕ respectively, $F_V = 156 \pm 5$MeV [19], M_V is the vector meson mass and ϵ_V and ϵ are the vector-meson and photon polarization vectors respectively, and e is taken positive.

The axial-vector meson coupling to VP can be expressed [8] as

$$t_{AVP} = g_{AVP} \, \epsilon_A \cdot \epsilon_V \tag{2}$$

where ϵ_A is the axial-vector meson polarization vector. The couplings g_{AVP} are obtained in Ref. [8] by evaluating the residues at the poles of the VP unitarized scattering amplitudes and are given in table VII of that reference. Note that in Ref. [8] the couplings are given in isospin base and for given $G-$parity states, hence the appropriate projection to charge base has to be done. In Ref. [8] no theoretical errors were quoted for these AVP couplings. However, for the purpose of evaluating the theoretical uncertainty in the calculations of the present work, we have estimated the uncertainties in these couplings in the following way: for the b_1 case, we have considered the change in the couplings due to a resonable uncertainty of 10% in the only free parameter of the model, the subtraction constant $a \sim -1.85$ (see Ref. [8] for details). We consider further uncertainties from changing f, as will be explained after Eq. (7). For the a_1 case, in Ref. [8] the mass obtained was 1011 MeV, somewhat below the nominal mass in the PDG [20], 1230 MeV. (Note however that the total width is $250 - 600$ MeV in the PDG, which gives an idea of the uncertainty in the mass). In Ref. [8], the mass was obtained with a value of $a = -1.85$. If we use the value $a = -1.1$ and $f = f_K$, we obtain a mass closer to the nominal of 1080 MeV, and it is not easy to get larger mass. In this case the coupling to $\rho\pi$, the dominant channel, is increased by $\sim 25\%$. From there, we get an idea of the uncertainties in the a_1 couplings.

This leads to the following radiative decay amplitudes for the tree level diagrams, (Fig. 1a)):

$$\begin{aligned} t_{b_1^+\to\pi^+\gamma} &= \frac{1}{3} e F_V \left(\frac{1}{M_\omega} g_{b_1\omega\pi} - \frac{\sqrt{2}}{M_\phi} g_{b_1\phi\pi} \right) \epsilon' \cdot \epsilon \\ t_{a_1^+\to\pi^+\gamma} &= -\frac{1}{\sqrt{2}} e F_V \frac{1}{M_\rho} g_{a_1\rho\pi} \epsilon' \cdot \epsilon \end{aligned} \tag{3}$$

In the evaluation of the loops an apparent problem arises given the large superficial divergence due to the loop momentum dependence of the vertices and the $q^\mu q^\nu / M_V^2$ terms of the vector meson propagators. However, we will explain in detail how one can circumvent this problem invoking gauge invariance and using a suitable Feynman parametrization of the loop integrals.

Since the only external momenta available are P (the axial-vector meson momentum) and k (the photon momentum), the general expression of the amplitude can be written as

$$T = \epsilon_{A\mu}\epsilon_\nu T^{\mu\nu} \tag{4}$$

with

$$T^{\mu\nu} = a\, g^{\mu\nu} + b\, P^\mu P^\nu + c\, P^\mu k^\nu + d\, k^\mu P^\nu + e\, k^\mu k^\nu \tag{5}$$

Note that, due to the Lorentz condition, $\epsilon_{A\mu}P^\mu = 0$, $\epsilon_\nu k^\nu = 0$, all the terms in Eq. (4) vanish except for the a and d terms. On the other hand, gauge invariance implies that $T^{\mu\nu}k_\nu = 0$, from where one gets

$$a = -d\, P \cdot k. \tag{6}$$

This is obviously valid in any reference frame, however, in the axial-vector meson rest frame and taking the Coulomb gauge for the photon, only the a term survives in Eq. (4) since $\vec{P} = 0$ and $\epsilon_0 = 0$. This means that, in the end, we will only need the a coefficient for the evaluation of the process. However, the a coefficient can be evaluated from the d term thanks to Eq. (6). The advantage of doing this is that there are few mechanisms contributing to the d term and by dimensional reasons the number of powers of the loop momentum in the numerator will be reduced, as will be clearly manifest from the discussion below.

Let us start by evaluating the diagram 1b) with the photon emitted from the pseudoscalar leg for the $b_1^+ \to \pi^+\gamma$ decay channel (the other channels are totally analogous). We will call this diagram type-b, in contrast with the type-c, with the photon attached to the vector-meson leg which will be evaluated later on, (see Fig. 1).

For the evaluation of this diagram we also need the VPP and $PP\gamma$ vertices. The VPP Lagrangian used is (see Ref. [21] for normalizations used)

$$\mathcal{L}_{VPP} = -i\frac{g}{\sqrt{2}}\langle V^\mu[\partial_\mu P, P]\rangle, \tag{7}$$

where V_μ and P are the usual $SU(3)$ matrices containing the vector and pseudoscalar mesons. In Eq. (7) $\langle ...\rangle$ means $SU(3)$ trace and $g = -M_V G_V/f^2$, where M_V is the vector meson mass, $G_V = 55 \pm 5$ MeV [19] and f is the pion decay constant that we take from 93 MeV to 1.15×93 MeV to take into account the uncertainty due to the use of f instead of f_K which could actually enter some of the expressions. These uncertainties in the parameters, together with the uncertainties in other couplings of the theory, will be taken into account later on in the evaluation of the theoretical uncertainties of our results.

The $PP\gamma$ vertex is easily obtained from the lowest order $ChPT$ Lagrangian [22]

$$\mathcal{L} = \frac{f^2}{4}\langle D_\mu U^\dagger D^\mu U\rangle \tag{8}$$

where the photon field appears in the covariant derivative.

The amplitude for the type-b mechanism (see Fig. 1b) for the $b_1^+ \to \pi^+\gamma$ reads:

$$
\begin{aligned}
-it_b &= -i\frac{1}{\sqrt{2}} g_{b_1 K^* K} \int \frac{d^4q}{(2\pi)^4}\, \epsilon_A^\mu \frac{i}{q^2 - m_K^2} \frac{i}{(q-k)^2 - m_K^2} \\
&\times \frac{i}{(P-q)^2 - m_{K^*}^2} \left(-g_{\mu\alpha} + \frac{(P-q)_\mu (P-q)_\alpha}{m_{K^*}^2} \right) \\
&\times i\frac{m_{K^*} G_V}{\sqrt{2} f^2} (k - q - p_\pi)^\alpha (-ie) \epsilon^\nu (q + q - k)_\nu \\
&= -\frac{1}{\sqrt{2}} g_{b_1 K^* K} e \frac{m_{K^*} G_V}{\sqrt{2} f^2}\, \epsilon_A^\mu \epsilon^\nu\, I_{\mu\nu}
\end{aligned} \tag{9}
$$

with

$$
\begin{aligned}
I_{\mu\nu} &= \int \frac{d^4q}{(2\pi)^4} \frac{1}{q^2 - m_K^2} \frac{1}{(q-k)^2 - m_K^2} \frac{1}{(P-q)^2 - m_{K^*}^2} \\
&\times \left(-(2k-q)_\mu - q_\mu \frac{[(P-q)\cdot(2k-2P) + (P-q)^2]}{m_{K^*}^2} \right) 2q_\nu .
\end{aligned} \tag{10}
$$

In Eq. (9), $g_{b_1 K^* K}$ is the coupling of the b_1 to the $K^*\bar{K}$ and $\bar{K}^* K$ G-parity positive combination as defined in Ref. [8]. By looking at Eq. (10) one can see that in the worst case the loop integral, as it is written, is quadratically divergent. At this point, we can take advantage of the fact that we only need to evaluate the contribution to the d term of Eq. (5), as explained above. In fact, the most divergent term, the one with $(P-q)^2$, does not contribute to the that term. Indeed, we can write

$$
(P-q)^2 = (P-q)^2 - m_{K^*}^2 + m_{K^*}^2, \tag{11}
$$

and then the two first addends of the right hand side of the above equation give

$$
\int \frac{d^4q}{(2\pi)^4}\, \frac{(P-q)^2 - m_{K^*}^2}{(P-q)^2 - m_{K^*}^2}\, \frac{1}{q^2 - m_K^2} \frac{1}{(q-k)^2 - m_K^2}\, q_\mu q_\nu, \tag{12}
$$

which does not depend explicitly on P, since the $(P-q)^2 - m_{K^*}^2$ cancels the propagator where the P appears and, therefore, this integral cannot give contribution to the d term. Hence, for the purpose of evaluating the $k_\mu P_\nu$ contribution, Eq. (10) can be written as

$$
\begin{aligned}
I_{\mu\nu} &= \int \frac{d^4q}{(2\pi)^4} \frac{1}{q^2 - m_K^2} \frac{1}{(q-k)^2 - m_K^2} \frac{1}{(P-q)^2 - m_{K^*}^2} \\
&\times \left(-4k_\mu + 2q_\mu \left[1 - \frac{(P-q)\cdot(2k-2P) + m_{K^*}^2}{m_{K^*}^2} \right] \right) q_\nu
\end{aligned} \tag{13}
$$

which has one power less in the variable q than Eq. (10). Next we use the Feynman parametrization to evaluate this integral and we will see that the contribution to the d term is convergent.

We use the identity

$$\frac{1}{abc} = 2\int_0^1 dx \int_0^x dy \frac{1}{[a+(b-a)x+(c-b)y]^3}. \tag{14}$$

By setting

$$\begin{aligned} a &= (P-q)^2 - m_{K^*}^2, \\ b &= q^2 - m_K^2, \\ c &= (q-k)^2 - m_K^2 \end{aligned} \tag{15}$$

and performing the change of variable

$$q = q' + [(1-x)P + yk], \tag{16}$$

we have

$$\begin{aligned} I_{\mu\nu} = 2\int_0^1 dx \int_0^x dy \int \frac{d^4q'}{(2\pi)^4} \frac{1}{(q'^2+s+i\varepsilon)^3} \Bigg[&-4k_\mu(q'_\nu + [(1-x)P_\nu + yk_\nu]) \\ &+ 2(q'_\mu + [(1-x)P_\mu + yk_\mu])(q'_\nu + [(1-x)P_\nu + yk_\nu]) \\ &\times \left(1 - \frac{(P-q'-[(1-x)P+yk])\cdot(2k-2P) + m_{K^*}^2}{m_{K^*}^2}\right)\Bigg], \end{aligned} \tag{17}$$

with

$$s = (1-x)(xM_{b_1}^2 - m_{K^*}^2 - 2yP\cdot k) - xm_K^2. \tag{18}$$

However, in Eq. (17), all the terms that contribute to the d coefficient are finite. Hence, in the end, the evaluation of the amplitude of the type-b diagram is completely finite, and gives:

$$\begin{aligned} t_b = &-\frac{1}{\sqrt{2}} g_{b_1 K^* K} e \frac{m_{K^*} G_V}{\sqrt{2} f^2} 2P\cdot k\, \epsilon_A \cdot \epsilon \\ &\times \int_0^1 dx \int_0^x dy \frac{1}{32\pi^2} \frac{1}{s+i\varepsilon} \left[-4(1-x) - 4y(1-x)\frac{(xP-yk)\cdot(k-P)}{m_{K^*}^2}\right] \end{aligned} \tag{19}$$

In the derivation of Eq. (19) from Eq. (17) we have used the relation between the a and d coefficients given by Eq. (6). We have also used that [23]

$$\int d^4q' \frac{1}{(q'^2+s+i\varepsilon)^3} = i\frac{\pi^2}{2}\frac{1}{s+i\varepsilon} \tag{20}$$

and that terms with odd powers of q' vanish when performing the integration, by symmetry reasons. It is also worth explaining a subtle cancellation which occurs between two logarithmic divergent pieces when deriving Eq. (19), as explained below:

In Eq. (17), apart from the terms which provide a finite contribution to the d-term, already considered in Eq. (19), there are two more terms which contribute to the d-term and which are logarithmically divergent. One of them goes as $yk_\mu q'_\nu q'_\alpha (k-P)^\alpha$. After the q' integration, this gives a term proportional to $-yk_\mu P_\nu$, since the $q'_\nu q'_\alpha$ gives a result proportional to $g_{\nu\alpha}$. The other term goes as $q'_\mu(1-x)P_\nu q'_\alpha(k-P)^\alpha$ and gives a term proportional to $(1-x)k_\mu P_\nu$ after the q' integration, with the same proportionality coefficient as in the other case. However after doing the x and y integration these two terms give the same result but with opposite sign. Hence these two possible sources of divergent contribution to the $k_\mu P_\nu$ cancel exactly among themselves. Therefore the expression of the amplitude in Eq. (19) is totally finite. It is worth stressing again the power of the technique used here to evaluate the amplitude coming from the type-b loops since, despite starting from a loop quadratically divergent, we have been able to get rid of all the divergences in an exact way.

At this point, it is worth noting that the numerical evaluation of the term proportional to $1/m_{K^*}^2$ in Eq. (19) is about 5% of the other term. This term comes from the last factor of Eq. (17) which essentially is due to the the $p_V^\mu p_V^\nu/{m_V}^2$ part of the vector meson propagator. Hence, the $1/{m_V}^2$ terms can be safely ignored in the evaluation of the type-c diagram. This approximation is expected to be very accurate since, advancing some results, the type-c diagrams will be found to be very small compared to the type-b and hence the $1/{m_V}^2$ is a small piece of a diagram contributing little to the radiative decay width. Nonetheless, we will include later on this uncertainty in the theoretical error analysis.

Now we evaluate the amplitude corresponding to the type-c diagram, Fig. 1c).

We also need in these case the $VV\gamma$ vertex that we get from gauging the charged vector meson kinetic term

$$\mathcal{L} = -\frac{1}{2} F^\dagger_{\mu\nu} F^{\mu\nu} \tag{21}$$

with $F^{\mu\nu} = \partial^\mu V^\nu - \partial^\nu V^\mu$ with the minimal coupling substitution $\partial_\mu \to \partial_\mu + iqA_\mu$.

After neglecting the $1/{m_V}^2$ term of the vector meson propagator by the reasons explained above, we have:

$$-it_c = \frac{1}{\sqrt{2}} g_{b_1 K^* K} e \frac{m_{K^*} G_V}{\sqrt{2} f^2}\, \epsilon_A^\mu \epsilon^\nu\, J_{\mu\nu} \tag{22}$$

with

$$\begin{aligned} J_{\mu\nu} = \int \frac{d^4q}{(2\pi)^4} \frac{1}{q^2 - m_{K^*}^2} \frac{1}{(q-k)^2 - m_{K^*}^2} \frac{1}{(P-q)^2 - {m_K}^2} \\ \times \left[2q_\nu (2P-k-q)_\mu - q\cdot(2P-k-q) g_{\mu\nu} - (q-k)_\mu (2P-k-q)_\nu \right]. \end{aligned} \tag{23}$$

After keeping only the terms contributing to $k_\mu P_\nu$, doing the Feynman parametrization and using the relation of Eq. (6) the final expression of the amplitude coming from the type-c diagram is

$$t_c = -\frac{1}{\sqrt{2}} g_{b_1 K^* K} e \frac{m_{K^*} G_V}{\sqrt{2} f^2} 2P\cdot k\, \epsilon_A \cdot \epsilon \int_0^1 dx \int_0^x dy \frac{1}{32\pi^2} \frac{1}{s' + i\varepsilon} \left[y(1-x) - 3x + 2y + 1 \right] \quad (24)$$

with

$$s' = (1-x)(xM_{b_1}^2 - {m_K}^2 - 2yP\cdot k) - x m_{K^*}^2. \quad (25)$$

Despite the smallness of the terms coming from the $1/{m_V}^2$ term of the vector meson propagator in the type-b mechanism, it is worth mentioning a technicality regarding the cancellations of the divergences had we evaluated these terms in the type-c loop. If one keeps these $1/{m_V}^2$ terms in the vector-meson propagators one obtains that the terms with $1/{m_V}^4$ do not contribute to the $d\, k^\mu P^\nu$ term and there remains a logarithmic divergence proportional to $1/{m_V}^2$. This divergence should be expected to cancel had one included suitable tadpoles which could cancel the offshellness of the momentums of the vector-meson in the loops, in a similar way to what was shown in [24], where the factorization of the $\vec{q}^{\,2}$ terms in the loop was justified. For the same reasons, this factorization was also used in [8]. Should one take this prescription here, the $1/{m_V}^2$ terms would be also very small. In any case we will make a conservative estimate of the errors induced by considering these terms in one way or another. By knowing that the contribution to the width of the type-c loop diagram is one order of magnitude smaller than that of the type-b one, and that the changes found for the loop of type-b are of the order of 5%, an estimate of 10% error of the radiative width coming from these considerations is a safe estimate.

Adding both type-b and type-c loops, we have:

$$\begin{aligned} t_{loops} = & -\frac{1}{\sqrt{2}} g_{b_1 K^* K} e \frac{m_{K^*} G_V}{\sqrt{2} f^2} 2P\cdot k\, \epsilon_A \cdot \epsilon \int_0^1 dx \int_0^x dy \frac{1}{32\pi^2} \\ & \times \left(\frac{-4}{s + i\varepsilon} (1-x)[1 + y(xP - yk)\cdot(k-P)/m_{K^*}^2] \right. \\ & \left. + \frac{1}{s' + i\varepsilon} [y(1-x) - 3x + 2y + 1] \right). \end{aligned} \quad (26)$$

Another possible diagram with the photon directly emitted from the VPP vertex, which is needed to ensure gauge invariance of the set of diagrams, does not give contribution to the d coefficient since the vertices involved are both of the type $\epsilon' \cdot \epsilon$, with ϵ' either the vector or axial-vector meson polarization vector. Therefore there is no k momentum dependence either in the vertices or in the propagators and hence the integration cannot give contribution to the $k_\mu P_\nu$ structure.

Concerning the $a_1^+ \to \pi^+ \gamma$ decay, the evaluation is totally analogous to the previous one. The amplitude from the $K^* K$ loops, when adding both type-b and -c mechanisms is:

$$t_{loops}^{(K^* K)} = -\frac{1}{\sqrt{2}} g_{a_1 K^* K} e \frac{m_{K^*} G_V}{\sqrt{2} f^2} 2P\cdot k\, \epsilon_A \cdot \epsilon \int_0^1 dx \int_0^x dy \frac{1}{32\pi^2}$$

$$\times \left(\frac{-4}{s+i\varepsilon}(1-x)[1+y(xP-yk)\cdot(k-P)/m_{K^*}^2] \right.$$
$$\left. - \frac{1}{s'+i\varepsilon}[y(1-x)-3x+2y+1] \right) \quad (27)$$

where one has to change m_{b_1} by m_{a_1} in the evaluation of s and s' in Eqs. (18) and (25). Note the relative minus sign in the terms with s' of Eq. (27) with respect to Eq. (26). This is due to the fact that, as we mentioned above, the b_1 couples to the positive $G-$parity combination $(\bar{K}^*K + K^*\bar{K})$ while the a_1 couples to the negative $G-$parity combination $(\bar{K}^*K - K^*\bar{K})$.

In the a_1 case there is also the possibility of having ρ and π in the loops. This mechanism gives:

$$t_{loops}^{(\rho\pi)} = g_{a_1\rho\pi} e \frac{m_\rho G_V}{\sqrt{2}f^2} 2P\cdot k\, \epsilon_A\cdot\epsilon \int_0^1 dx \int_0^x dy \frac{1}{32\pi^2}$$
$$\times \left(\frac{-4}{s+i\varepsilon}(1-x)[1+y(xP-yk)\cdot(k-P)/{m_\rho}^2] \right.$$
$$\left. - \frac{1}{s'+i\varepsilon}[y(1-x)-3x+2y+1] \right) \quad (28)$$

where one has to change m_{b_1} by m_{a_1}, m_{K^*} by m_ρ, and m_K by m_π in the evaluation of s and s' in Eqs. (18) and (25).

The expression of the radiative decay width in the axial-vector meson rest frame is

$$\Gamma(M_A) = \frac{|\vec{k}|}{12\pi M_A^2}|T|^2 \quad (29)$$

where M_A stands for the mass of the decaying axial-vector meson and T is the sum of the amplitudes from the tree level and loop mechanisms removing the $\epsilon_A\cdot\epsilon$ factor.

On the other hand, giving the large width of the axial-vector meson, particularly for the a_1, it is appropriate to fold the expression of the amplitude with the mass distribution of the axial-vector resonance. Hence the final amplitude is obtained from the expression

$$\Gamma_{A\to P\gamma} = \mathcal{N}^{-1} \int_{(M_A-2\Gamma_A)^2}^{(M_A+2\Gamma_A)^2} (-)\frac{ds_A}{\pi}\, Im\left\{ \frac{1}{s_A - M_A^2 + iM_A\Gamma_A} \right\} \Gamma(\sqrt{s_A})\, \Theta(\sqrt{s_A}-\sqrt{s_A^{th}}) \quad (30)$$

where Θ is the step function, M_A and Γ_A are the nominal mass and total axial-vector meson width from the PDG [20] and s_A^{th} is the threshold for the dominant A decay channels. The errors quoted in the PDG for these magnitudes are taken into account in the error analysis. In Eq. (30), $\mathcal{N}$ is a normalization factor in the convolution integral obtained from the same integral as in Eq. (30) setting $\Gamma(\sqrt{s_A}) = 1$.

Once the formalism and the different vertices have been exposed, we are in a situation to address the possible contribution from mechanisms involving the π-a_1 mixing. The mixing of axial-vector and pseudoscalar mesons (or vectors and scalars) is possible through the

longitudinal component of the spin-1 propagator $P^\mu P^\nu/P^2$ [25–29]. In the Appendix we show that the diagrams corresponding to the present problem, involving this mixing, vanish in our formalism.

3 Results

		$\Gamma_{b_1\to\pi\gamma}$	$\Gamma_{a_1\to\pi\gamma}$
tree level	ϕ	23	–
	ω	16	–
	ρ	–	650
	total	76	650
loops	type-b K^*K	30	10
	type-b $\rho\pi$	–	96
	type-b total	30	136
	type-c K^*K	0.14	0.05
	type-c $\rho\pi$	–	0.7
	type-c total	0.14	1.02
	K^*K	34	8.7
	$\rho\pi$	–	102
	total loops	34	137
total this work		210 ± 40	460 ± 100
experiment		230 ± 60 [30]	630 ± 246 [31]

Table 1: Different contributions to the radiative decay widths. All the units are KeV.

In table 1 we show the different contributions to the partial decay width coming from the different mechanisms considered in the calculation. The theoretical error in the final results have been obtained by doing a Monte-Carlo sampling of the parameters of the model within their uncertainty and considering the uncertainties in the couplings discussed above. Note, however, that we have no freedom in the theory once the relevant parameters (actually a subtraction constant) are fixed. To these errors we add in quadrature the 10% from the arguments used above concerning the $1/{m_V}^2$ terms.

From the results one can see that the tree level contribution for the a_1 accounts for most of the decay width. However, for the b_1 the tree level by itself only accounts for about 1/3 of the experimental result, despite having two diagrams, ϕ and ω, that contribute to the tree level process. The smallness of the tree level contribution comes from the $-\sqrt{2}/3$ and 1/3 factor of the ϕ and ω coupling to the photon in comparison to the factor 1 for the ρ case present in the a_1 decay and also to the fact that the $a_1\rho\pi$ coupling obtained with the chiral unitary model [8] is larger than the $b_1\phi\pi$ and $b_1\omega\pi$.

Note also the constructive interference between the ϕ and ω diagrams despite the coefficient of the $V\gamma$ coupling having a different sign. This is so because the couplings of the

b_1 to $\rho\pi$ and $\omega\pi$ have also relative different sign. These relative signs are also a genuine non-trivial prediction of the chiral unitary model of Ref. [8].

Regarding the loop contribution, the total loop results for the b_1 and a_1 decays have a comparable absolute value. In the b_1 case it increases the decay rate to account very well for the observed experimental result, after interfering constructively with the tree level mechanism. Note that the most important contribution from the loops comes from the type-b mechanisms (see Fig. 1*b*). Particularly, for the a_1 case the dominant contribution to the loops come from the $\rho\pi$ loops.

It is worth stressing the important role of the interferences among the different terms to give the final result. The interferences depend essentially on the sign of the couplings and the imaginary part of the loop functions. The values and relative signs of the AVP couplings are non-trivial predictions of the chiral unitary model of Ref. [8] and hence, the agreement of our calculated radiative decay widths with experiment gives support to the model of Ref. [8] and, hence, the dynamical nature of these axial-vector resonances.

4 Conclusions

We have studied here the radiative decays $a_1^+ \to \pi^+\gamma$ and $b_1^+ \to \pi^+\gamma$ which had proved problematic before in several approaches. The novelty which allowed us to obtain a simultaneous good description of both decays was the consideration of the a_1 and b_1 axial vectors as dynamically generated resonances within the context of unitarized chiral perturbation theory. Because of that we found important loop contributions that were essential in reproducing the experimental values. Technically, it is particularly rewarding to see that, by invoking gauge invariance, the calculation is simplified and the relevant loops are shown to be convergent despite their large superficial degree of divergence. The nature of the resonances as quasibound states of meson and vector-meson states reverted into a loop contribution which provided a substantial contribution to the radiative amplitudes, particularly to the one of the b_1 radiative decay.

One might think that loop contributions could have been considered without resorting to the concept of a dynamically generated resonance, by simply taking the couplings of the resonance to their decay channels. However, for the important case of the b_1 we found that the contribution of the $\omega\pi$ loop vanished and the relevant contribution was coming from $\bar{K}K^*$ and $\bar{K^*}K$ which is a closed decay channel (up to the width of the states) and for which there is no valuable experimental information. The chiral unitary approach provides directly such couplings with definite signs since these states are a part of the building blocks of the resonances in the coupled channel approach. Similarly, with the use of a phenomenological Lagrangian, like the one of Ref. [13], one could get such couplings, but these are based on $SU(3)$ symmetry which is actually broken when one generates dynamically resonances with a nonperturbative approach like the one in Ref. [8]. One example of relevance to the present case is that, with the phenomenological Lagrangian, the $b_1 \to \phi\pi$ coupling is forbidden while in our case, the nonperturbative treatment of the problem, involving many iterative loops, generates a finite coupling that is dominant in

the tree level contribution of $b_1 \to \pi\gamma$ (see Table 1).

The fact that we obtain a good description of the two radiative decay rates for the first time provides support for the idea of the axial vector mesons as dynamically generated states within chiral dynamics. Other tests could follow as we get increased and more accurate information on the axial vector mesons, and the findings of the present work should serve to stimulate efforts in this direction.

5 Appendix: Mechanisms related to the mixing of axial-vector and pseudoscalar mesons

In addition to the terms discussed so far in this paper, we could have terms involving the mixing of the axial-vector and pseudoscalar mesons [25–29], through the longitudinal component of the axial-vector resonance. In our case this occurs with a_1-π mixing, allowed by G-parity. The possible mechanisms involving this mixing in our scheme are given in Fig. 2. However, we shall demonstrate here that they vanish in our formalism.

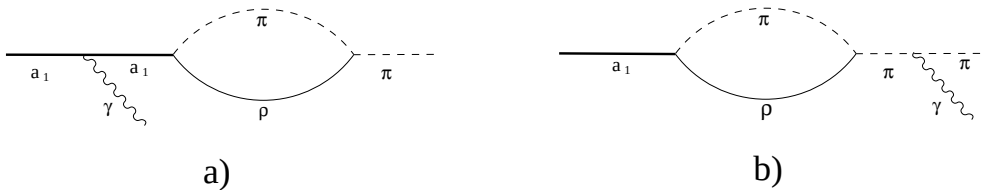

Figure 2: Diagrams involving the a_1-π mixing.

A free spin-1 massive meson propagator can be written as

$$\frac{-g^{\mu\nu}+\frac{P^\mu P^\nu}{M^2}}{P^2-M^2}=\frac{-g^{\mu\nu}+\frac{P^\mu P^\nu}{P^2}}{P^2-M^2}+\frac{P^\mu P^\nu}{M^2P^2} \tag{31}$$

where in the second term of the equality a separation has been done in terms of a transverse part ($-g^{\mu\nu}+\frac{P^\mu P^\nu}{P^2}$) and a longitudinal one ($P^\mu P^\nu$). Note that the pole of the particle appears only in the transverse part.

In our formalism, the axial-vector resonance is dynamically generated from the VP interaction and is associated to the poles of the scattering matrix. In the Appendix B of Ref. [8] we made explicitly the separation into transverse and longitudinal part, with the result that the poles appeared only in the transverse part of the amplitude. There we found for $T_{VP\to V'P'}$

$$T=\epsilon_\mu\epsilon'_\nu\left[\frac{Vb}{1-b}\left(g^{\mu\nu}-\frac{P^\mu P^\nu}{P^2}\right)+\frac{Vc}{1-c}\frac{P^\mu P^\nu}{P^2}\right] \tag{32}$$

where P is the total momentum of the VP system and ϵ, ϵ', the polarizations of the two vector mesons. In Eq. (32), c is very small compared to b and of opposite sign, such that

there are no poles in the longitudinal part. If we consider also a_1-π mixing, we would have to add terms like in Fig. 3 to our VP amplitude.

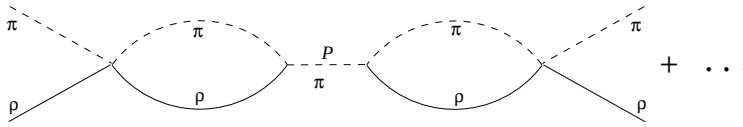

Figure 3: Extra contributions to the $VP \to VP$ interaction involving the a_1-π mixing

The loop function appearing in Fig. 3 has the structure $J(P^2)P^\mu$. The sum of terms in Fig. 3 renormalizes the longitudinal part of Eq. (32) which is changed to

$$\frac{Vc}{1-c-\frac{\beta J^2(P^2)}{P^2-m^2}}\frac{P^\mu P^\nu}{P^2} = \frac{Vc(P^2-m^2)}{(1-c)(P^2-m^2)-\beta J^2(P^2)}\frac{P^\mu P^\nu}{P^2} \tag{33}$$

where m is the pion mass. The amplitude has the unphysical feature of providing a pole related to the pion pole (close to m^2 if β is small). The way to remove this unphysical behaviour of the longitudinal part is to demand that $J(P^2=m^2)=0$, which also appears in other formalism [28]. In other works [29] it is shown explicitly that the renormalized full vector meson propagator contains only one pole which does not show up in the longitudinal part.

The contribution of the mechanisms of Fig. 2 in our formalism would have to be considered through the a_1 pole of the amplitudes of Fig. 4

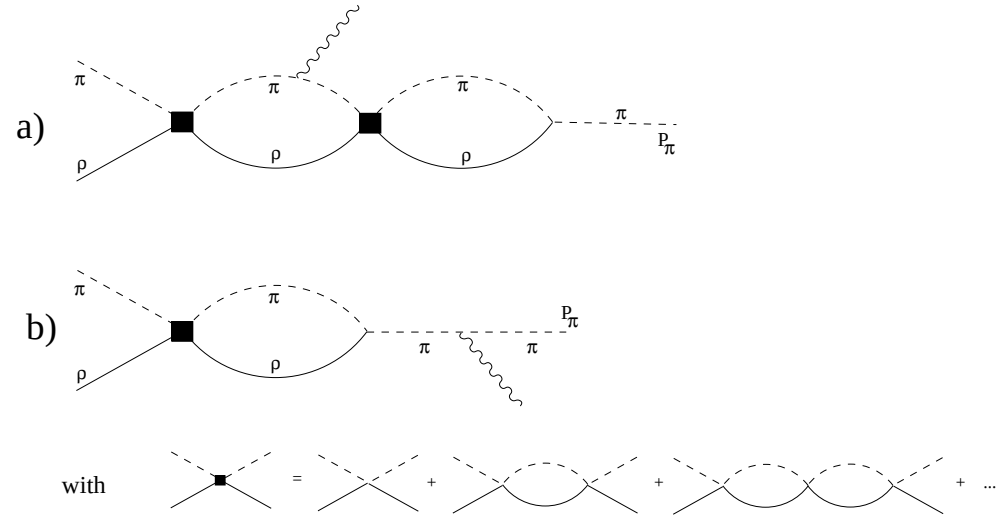

Figure 4: Mechanisms of Fig. 2 in the dynamical formalism

Diagram Fig. 4a), with the photon emitted either from the pseudoscalar or the vector in the loop, is proportional to $J(P_\pi^2=m^2)$ and hence vanishes.

Diagram 4b) is more subtle. The amplitude is proportional to

$$\epsilon_\mu(\rho)\left[\frac{Vb}{1-b}\left(g^{\mu\nu}-\frac{P^\mu P^\nu}{P^2}\right)+\frac{Vc}{1-c-\frac{\beta J^2(P^2)}{P^2-m^2}}\frac{P^\mu P^\nu}{P^2}\right]J(P^2)P^\nu$$
$$=\epsilon_\mu(\rho)P^\mu J(P^2)\frac{Vc}{1-c-\frac{\beta J^2(P^2)}{P^2-m^2}} \tag{34}$$

which has filtered the longitudinal part of the amplitude. Furthermore, the procedure we have followed to evaluate the coupling of a_1 to $\pi\gamma$ is equivalent to calculating the residue of the $\pi\rho \to \pi\gamma$ amplitude and dividing by the $a_1 \to \pi\rho$ coupling [32]. The residue of Eq. (34) at the resonance pole ($b = 1$) is zero and hence the mechanism of Fig. 4b) also vanishes at the a_1 pole.

Acknowledgments

We would like to express our thanks to Hideko Nagahiro who checked our calculations and help us to improve them. This work is partly supported by DGICYT contract number FIS2006-03438, the Generalitat Valenciana and the JSPS-CSIC collaboration agreement no. 2005JP0002. This research is part of the EU Integrated Infrastructure Initiative Hadron Physics Project under contract number RII3-CT-2004-506078.

References

[1] J. A. Oller, E. Oset and A. Ramos, Prog. Part. Nucl. Phys. **45** (2000) 157

[2] J. A. Oller and E. Oset, Nucl. Phys. A **620**, 438 (1997) [Erratum-ibid. A **652**, 407 (1999)].

[3] J. A. Oller, E. Oset and J. R. Pelaez, Phys. Rev. D **59** (1999) 074001 [Erratum-ibid. D **60** (1999) 099906].

[4] N. Kaiser, Eur. Phys. J. A **3** (1998) 307.

[5] V. E. Markushin, Eur. Phys. J. A **8** (2000) 389.

[6] J. Nieves and E. Ruiz Arriola, Phys. Lett. B **455** (1999) 30.

[7] M. F. M. Lutz and E. E. Kolomeitsev, Nucl. Phys. A **730** (2004) 392.

[8] L. Roca, E. Oset and J. Singh, Phys. Rev. D **72** (2005) 014002.

[9] L. S. Geng, E. Oset, L. Roca and J. A. Oller, Phys. Rev. D **75** (2007) 014017.

[10] L. Xiong, E. V. Shuryak and G. E. Brown, Phys. Rev. D **46** (1992) 3798.

[11] K. Haglin, Phys. Rev. C **50** (1994) 1688.

[12] G. Ecker, J. Gasser, A. Pich and E. de Rafael, Nucl. Phys. B **321** (1989) 311.

[13] L. Roca, J. E. Palomar and E. Oset, Phys. Rev. D **70** (2004) 094006.

[14] J. L. Rosner, Phys. Rev. D **23** (1981) 1127.

[15] J. L. Lucio Martinez and J. Pestieau, Phys. Rev. D **42** (1990) 3253.

[16] F. E. Close, N. Isgur and S. Kumano, Nucl. Phys. B **389** (1993) 513.

[17] E. Marco, S. Hirenzaki, E. Oset and H. Toki, Phys. Lett. B **470**, 20 (1999).

[18] J. A. Oller, Phys. Lett. B **426** (1998) 7.

[19] J. E. Palomar, L. Roca, E. Oset and M. J. Vicente Vacas, Nucl. Phys. A **729** (2003) 743.

[20] W. M. Yao *et al.* [Particle Data Group], J. Phys. G **33** (2006) 1.

[21] J. E. Palomar and E. Oset, Nucl. Phys. A **716** (2003) 169.

[22] J. Gasser and H. Leutwyler, Nucl. Phys. B **250** (1985) 465.

[23] F. Mandl and G. Shaw, Quantum Field Theory, John Wyley and Sons, 1984

[24] D. Cabrera, E. Oset and M. J. Vicente Vacas, Nucl. Phys. A **705** (2002) 90.

[25] D. Ebert and H. Reinhardt, Nucl. Phys. B **271** (1986) 188.

[26] M. Nowakowski and A. Pilaftsis, Z. Phys. C **60** (1993) 121.

[27] H. G. J. Veltman, Z. Phys. C **62** (1994) 35.

[28] A. E. Kaloshin, Phys. Atom. Nucl. **60** (1997) 1179 [Yad. Fiz. **60N7** (1997) 1306].

[29] G. Lopez Castro, J. L. Lucio and J. Pestieau, Int. J. Mod. Phys. A **11** (1996) 563.

[30] B. Collick *et al.*, Phys. Rev. Lett. **53** (1984) 2374.

[31] M. Zielinski *et al.*, Phys. Rev. Lett. **52** (1984) 1195.

[32] T. Hyodo, S. Sarkar, A. Hosaka and E. Oset, Phys. Rev. C **73** (2006) 035209 [Erratum-ibid. C **75** (2007) 029901].